AIAA Aviation 2015
22-26 June 2015, Dallas, Texas
21st AIAA/CEAS Aeroacoustics Conference

System Noise Prediction of the DGEN 380 Turbofan Engine

Jeffrey J. Berton*
NASA Glenn Research Center, Cleveland, Ohio 44135

The DGEN 380 is a small, separate-flow, geared turbofan. Its manufacturer, Price Induction, is promoting it for a small twinjet application in the emerging personal light jet market. Smaller, and producing less thrust than other entries in the industry, Price Induction is seeking to apply the engine to a 4- to 5-place twinjet designed to compete in an area currently dominated by propeller-driven airplanes. NASA is considering purchasing a DGEN 380 turbofan to test new propulsion noise reduction technologies in a relevant engine environment. To explore this possibility, NASA and Price Induction have signed a Space Act Agreement and have agreed to cooperate on engine acoustic testing. Static acoustic measurements of the engine were made by NASA researchers during July, 2014 at the Glenn Research Center. In the event that a DGEN turbofan becomes a NASA noise technology research testbed, it is in the interest of NASA to develop procedures to evaluate engine system noise metrics. This report documents the procedures used to project the DGEN static noise measurements to flight conditions and the prediction of system noise of a notional airplane powered by twin DGEN engines.

Nomenclature

c	=	speed of sound	w	=	objective function weighting factor
D	=	directivity distribution function	x	=	empirical calibration variable
f	=	frequency	α	=	jet convection correlation factor
F	=	Fresnel number	Δ	=	Fresnel number characteristic length
G	=	tip-Mach-dependent fan noise term	θ	=	polar (yaw) emission angle, zero at inlet
H	=	spool-speed-dependent shaft noise term	λ	=	wavelength
k	=	convective amplification exponent	ρ	=	density
L	=	noise level	ω	=	jet noise density term exponent
M	=	Mach number	Subscripts:		
$\dot{m}$	=	mass flow rate	c	=	convective
N	=	shaft speed	e	=	effective
n	=	jet noise velocity term exponent	f	=	flight
O	=	optimization function	i	=	one-third octave band frequency index
p	=	pressure	H	=	high pressure spool
S	=	spectral distribution function	I	=	shielding insertion loss
T	=	temperature	L	=	low pressure spool
V	=	velocity	r	=	relative

I. Introduction

NASA uses a phased approach to develop propulsion noise reduction technologies. Early in the process, candidate ideas are screened for practicality, viability and safety, and their effectiveness is typically assessed analytically. More attractive technologies may be selected for further maturation using higher-order computational tools and, when appropriate, model-scale component testing in small laboratory facility rigs. When resources permit, the most promising technologies and concepts may be selected for additional testing in major facilities such as acoustic wind tunnels, static outdoor acoustic tests on a large engine, or even on experimental flight tests. Aerospace industry may choose to develop these technologies into service if a successful business case for the concept can be made.

*Aerospace Engineer, Propulsion Systems Analysis Branch, MS 5-11, senior member AIAA.

A small turbofan such as Price Induction's DGEN could serve as an experimental testbed and provide valuable information midway through NASA's technology maturation process. Its small size would imply relatively low acquisition and operating costs, adaptability to operate in multiple facilities, and flexibility in changing or adapting hardware (e.g., inlet, fan, duct, or nozzle components). A small engine testbed could also be used to aid research in disciplines other than noise, such as engine control systems, engine health monitoring, aeroelasticity experiments, and dynamic response, materials or hybrid-electric research. Indeed, a test bench of the DGEN 380 digital engine-control unit has already been acquired by Glenn for engine controls research. Data from this control system model is used for this task.

The DGEN 380 is a twin-spool, unboosted, separate-flow geared turbofan with a static thrust of up to 570lb at sea level. The design fan pressure ratio is low enough to allow a very high bypass ratio (7.6) for an engine this small. The 14in diameter fan is geared, and fan tip speeds are subsonic. The core turbomachinery consists of a radial compressor and high- and low-pressure axial turbines. The inlet and bypass exhaust ducts are hardwall with no acoustic treatment. The engine exhausts through a coannular plug nozzle. A cutaway view of the engine is shown in Figure 1.

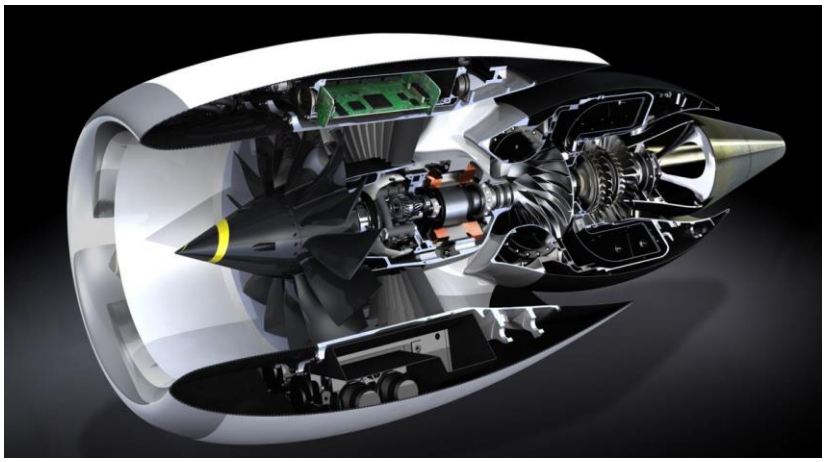

Figure 1. Cutaway view of the DGEN 380 turbofan
(Graphics: Price Induction).

Price Induction is promoting DGEN 380 and 390 series turbofans for a small twinjet application in the emerging light jet market. DGEN engines are smaller and produce less thrust than other entries offered, such as the Williams International FJ33 and the Pratt & Whitney PW600 series engines. Nomenclature for these new light jets seems ill-defined as of this writing; they are called Very Light Jets (VLJs) by some and Personal Light Jets (PLJs) by others, depending on characteristics such as gross weight, payload and performance. Available light jets are Eclipse Aviation's 500/550, Cessna's 510 Citation Mustang, and Embraer's Phenom 100, while Honda's HA-420 HondaJet is expected to be fully certified by the time this report is published. Light jet programs under development include Cirrus Aircraft's Vision SF50, and Diamond Aircraft's D-Jet (although the development of the D-Jet has been suspended). Price Induction intends to claim the PLJ market as their own since no other manufacturer offers a turbofan designed for aircraft operating in the regime currently dominated by propeller-driven airplanes under 25,000ft and 250ktas. Price Induction hopes to create a niche market with relatively affordable lightweight airplanes that are accessible to private pilots. Price induction is also targeting sales to aircraft engine maintenance schools as well as aerospace research organizations within government and academia.

Price Induction took a DGEN 380 on a promotional U.S. tour in July, 2014. The engine and its operating controls were mounted on a mobile flatbed truck platform and driven cross country. Prior to the tour, NASA and Price Induction Inc.,[*] signed a Space Act Agreement[1] and agreed to cooperate on engine acoustic testing. By the time the engine reached AIAA's Propulsion and Energy Forum and Exposition in Cleveland, Ohio, preparations had been made for a one-day acoustic test inside NASA Glenn's Aero-Acoustic Propulsion Laboratory.[2] The Laboratory is a large dome, sixty-five feet high and 130 feet in diameter. It is fitted with acoustic foam wedges, creating an anechoic environment down to 250Hz ideal for acoustic testing. The truck-mounted engine was located under an array of microphones designed for the dome's Nozzle Acoustic Test Rig, a freejet apparatus intended for jet noise research. Photos of the DGEN 380 parked inside the facility are shown in Figure 2 and in Figure 3. An inlet control device designed to reduce inflow distortion can be seen in Figure 3.

Narrowband acoustic spectra were measured at 24 emission angles and at six engine throttle settings. These measurements are the basis of this investigation. In the event that a DGEN turbofan becomes a NASA noise technology research testbed, it is in the interest of NASA to develop procedures to evaluate engine system noise metrics. This report documents the procedures used to project the DGEN static noise measurements to flight conditions and the prediction of system noise of a hypothetical airplane powered by twin DGEN engines.

[*]U.S.A. Price Induction Inc. is the North American office of Price Induction SA, a European SMB based in France.

Figure 2. Rear view of the DGEN 380 turbofan inside the NASA Glenn Aero-Acoustic Propulsion Laboratory anechoic dome *(Photo: NASA).*

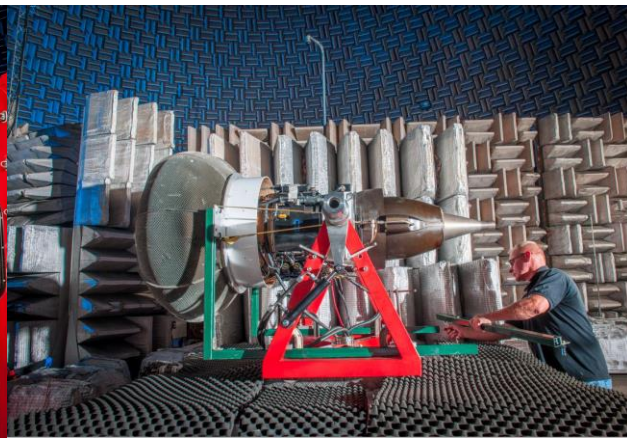

Figure 3. Portside view of the DGEN 380 turbofan, showing installation of the inlet control device *(Photo: NASA).*

II. Method of Analysis

A concept airplane suggested by Price Induction and shown in their promotional literature is a jet-powered variant of Cirrus Aircraft's propeller-driven SR22. The piston engine and propeller on the nose of the airplane is replaced by two DGEN 380 engines mounted on the fuselage. This notional 4-place personal light jet is illustrated in Figure 4. With a maximum takeoff gross weight of just 3400lb, a DGEN-powered SR22 variant is representative of the type of general aviation airplane targeted by Price Induction, and it is the airplane analytically modeled in this noise evaluation. Using a hypothetical Cirrus SR22 variant in this study is not meant to be an endorsement of the concept nor is it intended to detract from the development of Cirrus Aircraft's actual foray into the personal jet market: the larger, 7-place, 6000lb, single-engine Vision SF50.

The aircraft system noise metric chosen for this analysis is the Effective Perceived Noise Level, or EPNL. Under ICAO and FAA noise regulations (ICAO's Annex 16[3], or its FAA equivalent, Part 36[4]), any manufacturer seeking a noise type certificate for a non-experimental, civilian airplane equipped with DGEN turbofans would need to certify it as a jet-powered, subsonic airplane. Despite its small size, and despite that small, propeller-driven airplanes in its competitive market normally certify under much simpler noise regulations, a DGEN-powered airplane would be certified under regulations reserved for transport-category, large airplanes. Jet-powered airplanes regardless of size are required to certify using the EPNL noise metric and measurement procedures. The limits of the EPNL (i.e., how much noise an airplane is permitted to make) are regulated by authorities.

Figure 4: Notional, 4-place personal light jet powered by twin DGEN 380s; based on Cirrus Aircraft's SR22 propeller-driven airplane *(Graphics: Price Induction).*

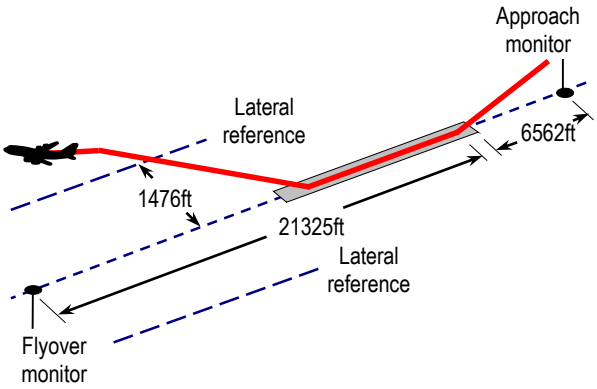

Figure 5: Noise certification monitor arrangement relative to takeoff and landing flight paths.

The basis of the EPNL is the perceived noise level, or PNL. The PNL is a weighted noise rating computed from 1/3rd octave band sound pressure levels, with particular emphasis given to levels at frequencies between 1kHz and 10kHz. An additional tone correction penalty is added to the PNL, forming the PNLT noise metric. During a noise certification test, spectral acoustic measurements are made as an airplane flies past three certification noise observation monitors on the ground (shown in Figure 5). Spectra are measured at half-second time intervals at each noise observation station. From these, PNLs and PNLTs are computed. The EPNL is determined from a PNLT versus time history. Thus the EPNL is a metric sensitive to level, frequency, tone content, and duration of a single airplane flyover event. In noise certification parlance, the cumulative, or algebraic, sum of the three certification EPNLs is often used to capture all three measurements.

The DGEN's noise spectra – measured statically by NASA and corrected for atmospheric absorption – can be analytically projected to simulated flight conditions by accounting for convective amplification and Doppler shift effects. Propagation phenomena such as spherical spreading, atmospheric absorption, and various ground effects can also be added to simulate a real airplane flyover event.

A sample noise spectrum acquired from the DGEN turbofan is shown in Figure 6. Narrowband power spectral densities emitted 118° from the inlet axis are plotted. The engine is operating at 96 percent of its maximum, sea level static, low-spool shaft speed (41,700rpm).* The spectrum is lossless and corrected for spreading to a one-foot distance. Fan tones at the fundamental blade passage frequency (BPF) and its harmonics are identified in the Figure. The fundamental fan tone is usually prominent, despite the cut-off fan design and the use of an inlet control device to eliminate inlet flow distortion. At most angles, another tone is present at the high-spool's shaft passage frequency (SPF_H). An additional prominent tone (with hay-stacking behavior) at much higher frequencies is created by the low-pressure turbine (LPT). When computing PNL, regulations only consider noise up to the 10,000Hz preferred one-third octave band center frequency. Acoustic content above 11,220Hz (the upper boundary frequency defined by the band filter required by ICAO) does not contribute to aircraft noise metrics. Thus, the 4BPF fan tone only contributes to certification noise at lower shaft speeds, or if Doppler effects in the aft quadrant are strong enough to shift it to lower frequencies. The strong turbine tone does not contribute to certification noise, even at lower engine power settings that would be used during approach. But since the turbine tone is distinct from fan tones, the DGEN could be a useful research testbed for the study of turbine noise.

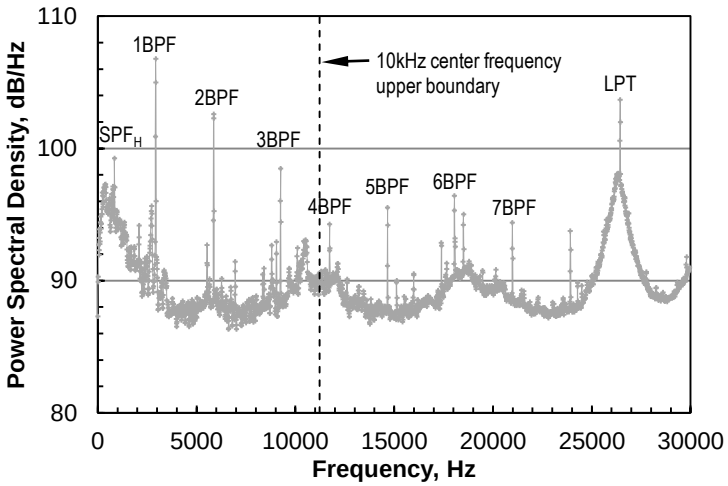

Figure 6. DGEN turbofan power spectral densities at 118° from inlet axis, operating at 96% of maximum low-spool shaft speed.

Perhaps the most expedient method for computing certification noise would be to use the measured engine spectra directly with a system noise analysis and propagation tool. Straightforwardly, the measured spectra could be analytically "flown" on a trajectory past observers on the ground. Propagation and ground effects could be applied and EPNLs computed for each observer. Convection and Doppler flight effects could be applied to improve accuracy.

However, there are problems with this approach. Engine behavior is different in flight than at ground level. Engine spool speeds, flow rates, temperatures and pressures – all of which influence engine noise – vary with altitude and airspeed. Correcting these properties with referred temperature and pressure is helpful, but imperfect. Without additional rigor, noise measured statically on the ground is not wholly representative of noise in flight.

In addition, jet mixing noise is a distributed source radiating along the axial plume of the exhaust. The microphones in the NASA facility ranged from 32ft to 57ft away from the engine: distances far enough to be considered in the acoustic far field, but not sufficiently distant to treat the entire exhaust plume as a point source radiating from the nozzle. A technique is required to relate microphone geometric angles to the engine with apparent angles to jet noise source locations.

*96 percent shaft speed was the highest engine power setting tested in the facility. 100 percent speed could not be achieved due to moderately-high ambient temperature on the day of the test.

Instead, empirical source noise prediction methods are derived and are used in place of measured noise. Noise surrogate models are constructed as empirical functions of engine state variables such as spool speed, flow rate, temperature and pressure. Empirical noise models are calibrated to the static spectra measured at NASA, and they are relied on to project spectra to arbitrary flight conditions. Engine state data are obtained from Price Induction's Virtual Engine Test Bench: an engine performance simulator built around the DGEN's engine control unit. In this study, polynomial response surfaces are created for engine state properties throughout the engine as functions of altitude, flight Mach number, and low-pressure spool speed. This approach ensures that engine noise predictions react properly to changes in altitude and airspeed.

Using noise surrogate models in place of actual spectra allows for removal of extraneous or spurious portions of the spectra that are not believed to be genuine engine noise, particularly at low frequencies where the acoustic dome facility is not sufficiently anechoic. Further, if the engine noise sources are separated and modeled individually, each source can easily be manipulated mathematically. This is useful when simulating the effects of adding noise reduction technology such as duct acoustic treatment (which would be applied only to fan noise), nozzle chevrons (a jet noise reduction technology) or when conducting a noise uncertainty analysis of each component as it relates to the overall system. Last, component noise modeling allows for the removal of engine noise sources that may be eliminated or reduced during manufacturing and would not be present in the final, production engine.

Engine noise modeling is discussed in detail immediately below. The measured spectra are corrected for atmospheric absorption. The levels of the lossless spectra can be adjusted to any distance using a spherical spreading correction (the actual distance to the microphone is used when deriving the jet noise method so that distributed source effects can be modeled). Each noise method is formulated in the one-third octave band paradigm, using decibels referenced to 20μPa. When computing certification noise, convection and Doppler effects in each source noise model are applied and spectra are projected to flight conditions appropriate for a DGEN-powered airplane. A trajectory analysis is performed for a small, notional, personal light jet to determine the approximate flight path past each noise certification monitor. In-flight spectra are fed into NASA's Aircraft Noise Prediction Program (ANOPP[5,6]) as user-supplied noise, propagation losses and ground effects are applied. and certification noise levels are computed.

1. Engine Noise Sources

Core noise predictions are based on a simple empirical expression[7] suggested by the Society of Automotive Engineers. Lossless core noise spectra (L_{Core}, in dB, as a function of frequency f and polar emission angle, θ) are expressed as a function of engine properties, namely the mass flow rate entering the combustor ($\dot{m}$), the change in total temperature through the combustor (ΔT_{Comb}) and the density of the flow entering the combustor (ρ_{Comb}):

$$L_{Core}(f,\theta) = 10\log_{10}\left\{ x_1 \frac{\dot{m}}{\dot{m}_{Ref}} \left[\frac{\Delta T_{Comb}}{T_{Ref}} \right]^2 \left[\frac{\rho_{Comb}}{\rho_{Ref}} \right]^2 \frac{D(\theta)\, S(f, x_2)}{\left[1 - M_f \cos\theta\right]^k} \right\} \tag{1}$$

The flow properties are rendered dimensionless with reference parameters. D is a dimensionless directivity function correcting levels for emission angle and S is a dimensionless function that accounts for spectral shaping and Doppler shift. In flight, levels are adjusted for the flight Mach number M_f with the term $1 - M_f \cos\theta$ raised to a convective amplification exponent, k (taken to be four for quadrupole emissions). The method defines core noise as direct and indirect unsteady combustion noise. Turbine noise is not included in the method, but in the DGEN engine it is at such high frequencies it is not expected to be relevant to certification noise. Spherical spreading corrections are applied afterwards.

The terms x_1 and x_2 are empirical calibration variables. Suggested values are given in the original reference and elsewhere, but in this study they are variables intended to fit the predictive model (with $M_f = 0$) to the measured static spectra. x_1 adjusts core noise spectra for amplitude, while x_2 adjusts for curvature. Fitment of spectra is discussed in the following section.

Fan noise predictions are based on an early empirical method developed by NASA,[8] but recalibrated for modern, wide-chord, low-pressure-ratio fans.[9] Acoustic power level is proportional to the mass flow rate entering the fan, the total temperature rise across the fan stage (ΔT_{Fan}), and an empirical function dependent on the relative (helical) fan rotor tip Mach number, $G(M_r)$. Lossless fan noise spectra L_{Fan} are given by

$$L_{Fan}(f,\theta) = 10\log_{10}\left\{ x_3 \frac{\dot{m}}{\dot{m}_{Ref}} \left[\frac{\Delta T_{Fan}}{T_{Ref}} \right]^2 G(M_r) \frac{D(\theta)\, S(f, x_{4-8})}{\left[1 - M_f \cos\theta\right]^k} \right\} \tag{2}$$

The method models broadband and rotor-stator discrete interaction tones separately. In addition to accounting for Doppler shift, the spectral function S assigns an additional level representing an interaction tone whenever the one-

third octave frequency span contains a multiple of the blade passage frequency. In other implementations of the method, additional terms are present to account for effects such as variable rotor-stator spacing, inlet guide vanes, and flow distortion. These terms, however, are omitted here since they reduce to constants and since fan noise is already adjusted using the calibration variables x_3 through x_8. In this instance, x_3 adjusts fan noise spectra for amplitude, x_4 adjusts for curvature, and x_5 through x_8 adjust the levels of the first four interaction tones.

Shaft acoustic power is based on an empirical function H, a polynomial regression dependent on high and low spool shaft speeds, N_H and N_L. L_{Shaft} is given by

$$L_{Shafts}(f,\theta) = 10\log_{10}\left\{ x_9 x_{10} H(N_L, N_H) \frac{D(\theta)\, S(f)}{\left[1 - M_f \cos\theta\right]^k} \right\} \tag{3}$$

The spectral function assigns levels when the one-third octave frequency span contains one or both shaft passage frequencies. It also accounts for Doppler shift. x_9 and x_{10} are used to make finer adjustments to shaft order tone levels unaccounted for by H.

Jet noise is modeled using a semi-empirical method developed by Stone.[10] The problem is approached by breaking overall jet noise into several virtual components, each accounting for different noise-generation mechanisms within the jet plume. Since both the core and bypass nozzles are subcritical throughout the takeoff regime, the jets are modeled as shock-free streams and shock-related jet noise components are ignored. Three turbulent mixing components are considered: 1) large-scale, merged-stream mixing noise (low-frequency content generated by large turbulent eddies several diameters downstream of the exit plane), 2) small-scale mixing noise (relatively high-frequency content generated at the exit plane of the nozzle by the jet-to-ambient shear layer), and 3) transitional, intermediate-scale mixing noise. The intermediate-scale noise is the most difficult component to characterize. It is predominantly caused by the inner shear layer at the interface between the streams of a coannular nozzle. The overall levels of the mixing noise components are functions of jet velocity, jet density, size of the jet, and the convective Mach number. Spectral shapes are characterized by Strouhal number functions. The general form of the three lossless mixing components is

$$L_{Jet}(f,\theta) = 10\log_{10}\left\{ x_{11} \left(V_e / c_{Ref}\right)^n \left(\rho / \rho_{Ref}\right)^\omega \frac{D(\theta_e)\, S(f,\theta_e)}{\left(1 + M_c \cos\theta\right)^2 + \alpha^2 M_c^2} \right\} \tag{4}$$

where V_e is an effective jet velocity (normalized by ambient sound speed to form an acoustic Mach number), n a velocity slope, ρ a fully-expanded jet density, and ω a variable density exponent. Each represents an appropriate value for the jet noise component being considered. θ_e is an effective polar emission angle dependent on jet velocity that accounts for refraction. Although jet noise source locations vary, they are assumed to vary similarly with jet velocity and can be correlated to the geometric emission angle. Each spectrum is adjusted to the distance from the nozzle to the microphone before calibration (refraction modeling is discussed in greater detail in Ref. 10). Stone found that better agreement with in-flight data could be obtained by eliminating the convection term $1 - M_f \cos\theta$ and relying upon only a convective Mach number M_c and an empirical convection constant α to account for the effects of simulated flight. All three mixing noise components are ganged together and adjusted by the calibration constant x_{11}.

2. Fitment of Spectra:

An optimizer is used to aid fitment of the noise models to the measurements. A composite objective function $O(\mathbf{x})$ is defined:

$$O(\mathbf{x}) = w_1 \frac{\sum_i \left(L_{i,data} - L_{i,model}\right)^2}{\sum_i \left(L_{i,data} - \bar{L}_{data}\right)^2} + w_2 \left(L_{TPN,data} - L_{TPN,model}\right)^2 \tag{5}$$

The first term is the residual sum of squares divided by the total sum of squares over all L_i sound pressure level observations of a spectrum. The first term, if driven to zero, would represent a perfect fit of noise models to the measured data, and it alone would suffice as an objective function. But neither the noise models nor the data are perfect representations of the system, so obtaining a perfect fit is difficult. Further, at least as important as matching the spectral shape is matching the frequency-independent tone-corrected perceived noise level (PNLT, given the notation L_{TPN}), since it is the metric used directly to compute certification EPNL. Given this, the squared difference of L_{TPN} is added as a second term in $O(\mathbf{x})$, with w_1 and w_2 used as weighting factors.

Of course a minimum, nonzero $O(\mathbf{x})$ does not result in a unique solution. Caution is warranted when using this logic to fit noise models. Generally, values of x should not stray too far from their nominal values. It is easy to envision a case where levels of one noise component are driven unrealistically high just to drive $O(\mathbf{x})$ a bit smaller, only to have a more realistic noise component overshadowed. Judicious limits should be set for values of x. This is discussed in greater detail in Section III.

3. Airframe and Installation:

Propulsion noise is combined with airframe noise appropriate for a Cirrus SR22 using the Fink method.[11] The method uses empirical functions to model noise spectra as functions of polar and azimuthal emission angles. Spectra are predicted for the SR22's trailing edge planform surfaces, landing gear and single-slotted flaps. The SR22 has fixed, non-retracting landing gear and no leading edge slats. The method uses gross airframe dimensions such as span, flap chord lengths, and gear configuration and dimensions; all of which may be obtained from a simple, open-literature, three-view aircraft drawing.

Noise shielding (also referred to as barrier attenuation or insertion loss) is an acoustic diffraction phenomenon where acoustic waves are attenuated when propagated past an impermeable barrier placed between the noise source and an observer. Shielding is particularly efficient when the observer is located in the "shadow region" where the noise source is obscured. The wing planform provides a shielding surface for the engine located above and behind the wing trailing edge. Airframe noise sources and jet noise – a distributed source generated downstream throughout the axial exhaust plume – are not shielded.

The method used to predict shielding is a simple empirical diffraction model based on asymptotic results of optical diffraction theory, originally proposed by Maekawa[12] and reproduced in many foundational acoustic textbooks. The analytic treatment of diffraction effects in this manner is common in aeroacoustic applications. Reliable, fast, and easy to implement, it has been coded into aircraft noise system prediction programs.

Maekawa proposed the shadow zone insertion loss relation:

$$L_I = 20\log_{10}\left(\sqrt{2\pi|F|}\Big/\tanh\sqrt{2\pi|F|}\right)+5 \qquad (6)$$

in dB, where F is the frequency-dependent Fresnel number ($2f\Delta/c$), whose characteristic length Δ is the difference between the shortest path around the barrier between the source and the observer and the source-observer distance directly through the barrier. For observers in the bright zone (F < -0.192), the attenuation is neglected, and for observers in the transition zone (-0.192 < F < 0), it is appropriate to replace the hyperbolic tangent with the trigonometric tangent. Although the above relation is intended for use with semi-infinite barriers, Maekawa suggested that superposition may be used for barriers of finite length and width, such as a wing planform.

III. Results and Discussion

1. Spectral results:

The noise models are calibrated to every spectrum acquired in the facility. With 24 polar emission angles (ranging from 36 to 145 degrees relative to the inlet axis), and six engine power settings (ranging from 47 percent to 96 percent of the maximum low-spool shaft speed), a dataset of 144 static spectra are available to perform a system noise assessment. Measured and modeled spectra at 138 degrees and at the highest power setting are plotted in Figure 7 for discussion.

Narrowband, lossless sound pressure levels for a virtual observer on a one foot radius are plotted using a frequency interval of 12.2Hz. Tone content at the high-spool shaft frequency and at the first three fan passage frequencies are easily seen in the narrowband data. The narrowband data are summed to a coarser, one-third octave band spectrum indicated by the symbols. Higher-frequency fan or turbine noise does not contribute to the analysis, since levels only at frequencies from 50Hz to 10kHz are used to compute noise certification metrics.

The calibrated spectra of fan, jet, core, and shaft noise models are also plotted. Fan and shaft noise levels are perhaps the easiest sources to identify and to calibrate. Both sources peak at

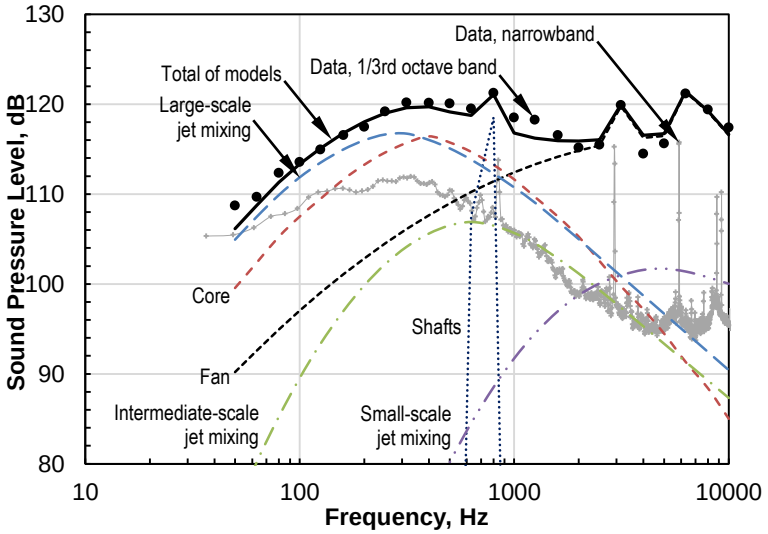

Figure 7. Measured and modeled lossless spectra at 138° from inlet axis, 96% of maximum low-spool shaft speed.

frequencies where no other significant noise sources exist, and their prominent tones are easily identified and can be used as a guide. Tone content, incidentally, is an anathema to applicants of noise type certificates and to airplane occupants. In many cases, DGEN fan tones contribute mightily to the PNLT metric, owing primarily to the heavy tone correction penalty assigned to high-frequency tones. Acoustic treatment applied to the inlet and bypass ducts could abate these tones.

From 50Hz to about 600Hz, individual broadband noise sources are not as easily identified. At frequencies peaking at about 400Hz, large-scale jet mixing noise and core noise coexist in some proportion. It is often difficult to tell when, or if, jet noise is masquerading as core noise or vice versa. One method to determine the contribution of core noise in a signal is to use source separation coherence techniques. During NASA's one-day test of the DGEN engine, a semi-infinite-tube transducer was mounted in the core tailpipe to measure pressure fluctuations in the exhaust. When an exhaust signal is analyzed along with signals from a companion microphone located in the far field, core noise can be educed. Coherent combustor broadband noise was detected up to about 500Hz using a two-signal coherent output power method.[13] Unfortunately due to limits on time and resources, the tests were restricted to just one aft angle. Generally, the experiment revealed the core noise method of Ref. 7 to overpredict core noise by approximately 11dB. Although this is a preliminary finding requiring further evaluation, it is helpful information when assigning values to jet and core noise calibration variables.

Another technique is to use lower engine throttle settings as a guide in setting core noise calibration variables. At low engine power, jet velocity – and jet noise – is quite low, so the presumption is that core noise is the most prominent low-frequency feature in the spectra. As engine power is increased and jet noise level rises (indeed, very dramatically, with velocity to the eighth power!), the physics-based source noise models are relied on to report the correct proportions of jet versus core noise. Both the source separation experiment result and low-power-setting data are used as guides in calibrating jet and core noise models.

In general, jet noise predictions are adjusted little, while core noise predictions are reduced. Still, without more rigor in separating core and jet noise, the results are lumped together when reporting component contributions to the certification noise level.

2. Airplane Trajectory:

Airplane trajectories and engine operating conditions have an important influence on certification noise. Airplane takeoff and landing trajectories are computed using an aircraft trajectory simulation tool. Engine thrust data collected from the DGEN digital control system and aerodynamics representative of a general aviation airplane are inputs to the trajectory analysis.

Trajectory data evaluated for a sea level field at 77°F are shown in Figure 8. Altitude above field elevation, true airspeed, and true thrust per engine are plotted against the distance from brake release. The trajectories are shown with takeoff and landing operations superimposed. For presentation purposes, the touchdown point on landing is coincident with the point of brake release on takeoff. Thrust for the noise

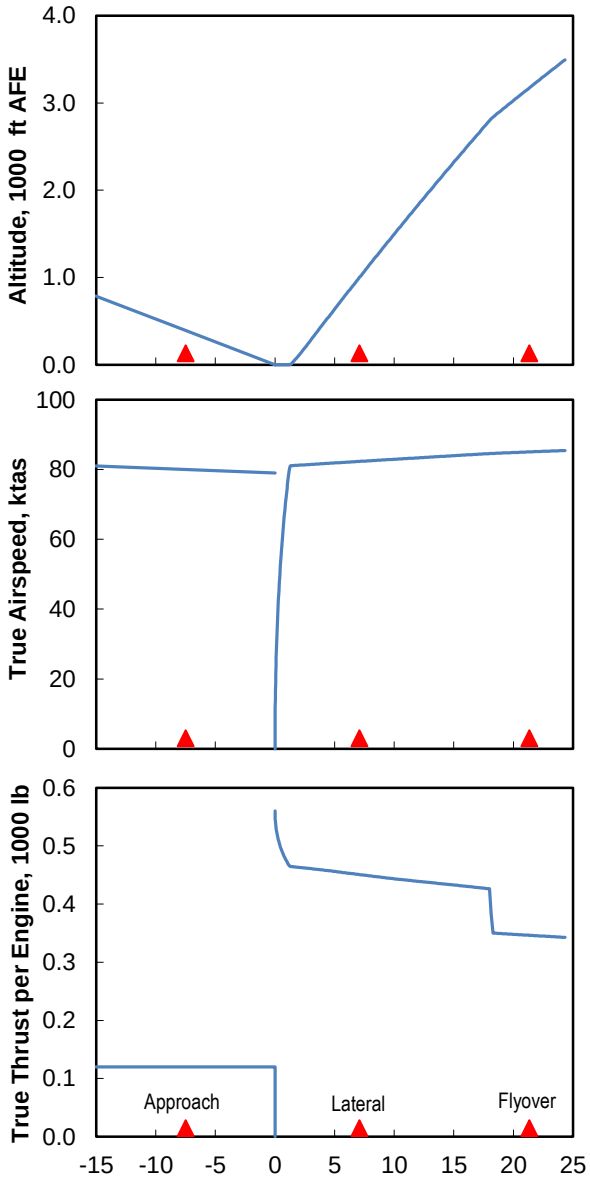

Figure 8. Departure and arrival trajectories.

abatement engine power cutback is set such that the climb gradient is zero with one engine inoperative, or four percent with both engines operating. It is completed at approximately 17,000ft from brake release. On approach, a three-degree glide slope is followed, the maximum landing weight is assumed, and the single-slotted flaps are extended. The engine thrust is set to a level that maintains a stable glide slope.

The triangular markers on each chart denote noise certification measurement locations. The approach microphone markers are shown in the figures at 6562ft behind the runway threshold, and approximately 7518ft behind the instrument landing system touchdown zone on the runway centerline. The monitor is located under the point of the approach path where the airplane is 394ft above ground level. The lateral microphone location lies along a sideline parallel to the runway displaced 1476ft from the extended runway centerline. It is located along the sideline across from the location where the airplane reaches an altitude of 1000ft above field elevation (i.e., the point where ground attenuation effects diminish and where maximum lateral noise is typically observed). The flyover microphone markers are shown in the figures at 21,325ft from brake release on the extended runway centerline.

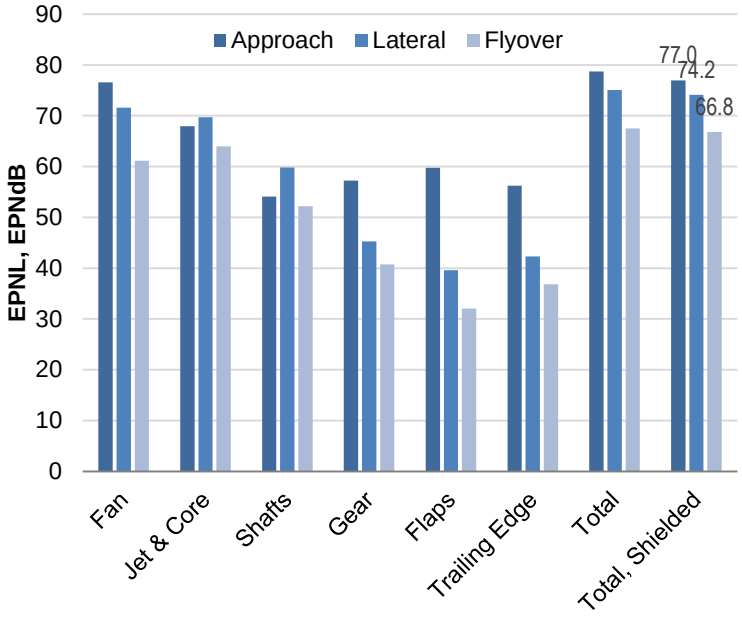

Figure 9. EPNL predictions.

3. Noise Certification Results:

Flight conditions and engine power settings neighboring each noise observation monitor are used as inputs to the calibrated noise models. Static component noise spectra are projected to flight conditions, summed in the vicinity of the airplane, and propagated to the ground using the ANOPP software. EPNLs at each observation station are determined from PNLT versus time histories at half-second time intervals. Component and total system EPNLs are shown in Figure 9. The effect of shielding is shown in the rightmost columns. Jet and core noise levels are not reported individually due to the spectral separation issues described earlier.

Fan noise dominates the approach and, to a lesser degree, lateral noise signatures. Jet and core noise dominate flyover noise and contribute to lateral noise. Shaft noise appears to play a minor role in lateral and flyover noise levels, but not at approach. Even if shaft noise sources could be identified and addressed during engine production, it would not significantly reduce certification noise. Airframe sources, even when taken together, contribute only a few tenths of an EPNdB to the approach level. Wing planform shielding effects – applied to fan, core and shaft noise – reduce EPNL by 1.7, 0.9 and 0.7 EPNdB at the approach, lateral and flyover locations, respectively.

Predicted noise levels of the notional DGEN 380 twinjet are plotted against maximum takeoff gross weight in Figure 10. The error bands surrounding the predictions represent one standard deviation of uncertainty determined by a Monte Carlo experiment discussed in the next section. Chapter 3 limits are shown for each certification location, and the anticipated Chapter 14 limit for twinjets is shown in the cumulative chart. Chapter 14 limits for aircraft of this size (under 55tonnes) are expected to debut on December 31, 2020. The predictions are also compared against published EPNLs of other aircraft.[14]

The notional DGEN twinjet is predicted to be remarkably quiet with respect to regulation limits as well as to other aircraft. It enjoys cumulative margins of 27.4 and 53.1 EPNdB to Chapter 14 and Chapter 4 limits, respectively.

4. Uncertainty Analysis:

Since the results are determined from a variety of largely-unknown elements, a Monte Carlo uncertainty analysis is performed to provide insight into the system model. Normally deterministic, the benchmark noise model is transformed into a stochastic model by replacing portions of its input data with continuous random values. A vector of input variables representing modeling unknowns is randomly permuted using probability distributions centered around the model's nominal values. The input variables subject to randomization are chosen by a top-down decomposition of the system noise problem.

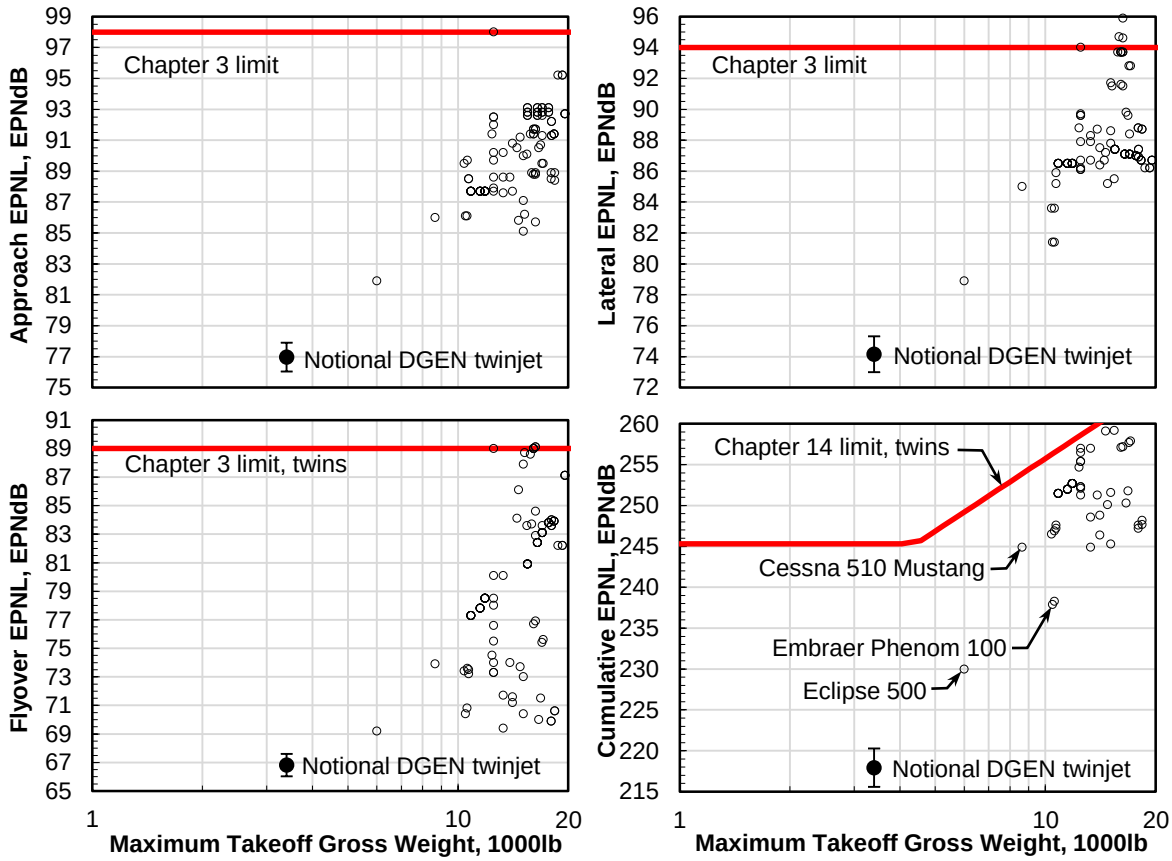

Figure 10. Notional DGEN twinjet noise predictions compared to certification data and Chapter 3 and Chapter 14 limits. Error bars represent one standard deviation in an uncertainty analysis.

Table 1. Uncertainty variables used in Monte Carlo experiment.

Variable	Mode	Model	Min	Max	Std. Dev.
Approach flight Mach no.	0.119	Triangular	0.112	0.126	-
Lateral flight Mach no.	0.123	Triangular	0.119	0.127	-
Flyover flight Mach no.	0.128	Triangular	0.120	0.150	-
Approach N_L setpoint	60%	Triangular	58%	62%	-
Lateral N_L setpoint	96%	Triangular	94%	100%	-
Flyover N_L setpoint	90%	Triangular	87%	93%	-
Approach angle of attack	6°	Triangular	5°	7°	-
Lateral angle of attack	6°	Triangular	5°	7°	-
Flyover angle of attack	6°	Triangular	5°	7°	-
Flyover altitude	3170ft	Triangular	2850ft	3490ft	-
Fan noise adjustment	0	Normal	-	-	1.0dB
Core noise adjustment	0	Normal	-	-	1.0dB
Shaft noise adjustment	0	Normal	-	-	1.0dB
Jet noise adjustment	0	Normal	-	-	1.0dB
Landing gear noise adjustment	0	Normal	-	-	1.5dB
Flap noise adjustment	0	Normal	-	-	1.5dB
Trailing edge noise adjustment	0	Normal	-	-	1.5dB
Ground specific flow resistance	291sl/s-ft^3	Triangular	233sl/s-ft^3	349sl/s-ft^3	-
Lateral attenuation adjustment	0	Triangular	-2dB	2dB	-
Wing area (shielding)	155ft^2	Uniform	0	200ft^2	-

These uncertainty variables are presented in Table 1. The variables are chosen to represent various effects that would certainly stray from mode values assumed for the benchmark case during the course of aircraft development. Randomly-changing variables represent the lack of knowledge of system characteristics, as well as the accuracy of (and uncertainty in) source noise prediction methods. Notably, atmospheric properties are not varied, despite their strong influence on atmospheric absorption and other phenomena. Since ICAO requires acoustic measurements to be corrected to standard acoustic day conditions, there is little reason to include ambient temperature or relative humidity in the experiment. There are no variables assigned to represent variations in wind, terrain, or airport elevation for similar reasons.

Since the airplane is notional, all trajectory-related variables are subject to variability. Engine power settings on approach and during the noise abatement thrust cutback are dependent on airplane weight, aerodynamics and regulations. These variables are allowed to change within limits judged reasonable using triangular distribution models. Each noise source is allowed to vary using normal distributions. Airframe noise sources are assigned somewhat more variability than propulsion sources since the airplane configuration is not precisely known. Ground specific flow resistance and lateral attenuation are environmental variables affecting noise during certification testing. Last, the wing planform shielding area is allowed to vary uniformly from zero (no shielding) to a maximum of 200ft^2. As wing area is varied, wing aspect ratio, taper ratio and sweep are held constant.

Table 2. Uncertainty statistics (in EPNdB).

Statistic	Approach	Lateral	Flyover	Cumulative
Benchmark case	77.0	74.2	66.8	217.9
Minimum of samples	74.3	70.6	64.4	209.5
Maximum of samples	80.5	78.1	69.7	226.4
Range of samples	6.2	7.6	5.3	17.0
Mean of samples	77.3	74.6	66.8	218.7
Standard deviation	0.9	1.2	0.8	2.3

The three certification EPNLs comprise the set of stochastic output response variables. A single analysis requires about three minutes to execute on a contemporary office computer. The Monte Carlo problem lends itself to concurrent parallelization, so the analyses may be multi-threaded across several platforms. A robot is easily constructed to modify a template input file, permute its contents with randomly-generated inputs, and run the analysis. The noise model is interrogated eight thousand times. Results of the uncertainty experiment are shown in Figure 11 for cumulative EPNL. Statistics for the experiment are presented in Table 2.

After eight thousand samples, there do not appear to be multiple modes or truncations in any of the histograms. Skew and kurtosis are not major factors. As is the case in any uncertainty experiment, the spread of the data perhaps is the most revealing. The standard deviations are rather small; on the order of only 1 EPNdB at each observer.

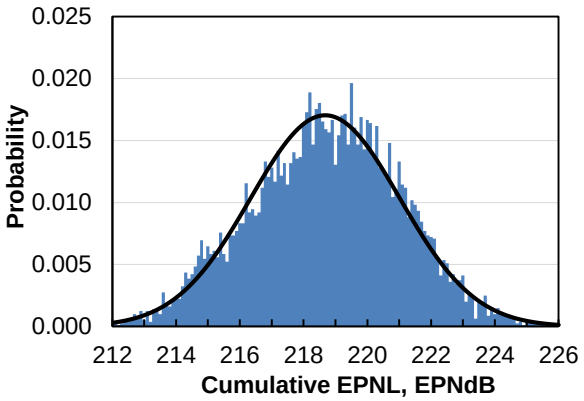

Figure 11. Monte Carlo uncertainty analysis of cumulative EPNL. Histogram and normal distribution generated from 8000 samples and bin span of 0.1 EPNdB.

IV. Conclusions

Static noise measurements of a Price Induction DGEN 380 turbofan collected at NASA Glenn Research Center are used to develop propulsion noise prediction models. Calibrated to measured data, the models represent the actual noise level of a DGEN engine, but embedded physics-based behavior allows them to react properly to changing engine state and flight conditions. The models are used to analytically project noise spectra to flight conditions and to predict system noise of a notional airplane powered by twin DGEN engines. The DGEN is a quiet turbofan, owing not only to its small size, but also to its design. The gearbox allows the fan to spin more slowly than the low-pressure turbine. With the fan generating less bypass duct pressure, turbine power can be used to drive the bypass ratio very high for

this class of engine. Relatively low fan speeds and low jet velocities result in a very low propulsion noise signature. A notional DGEN twinjet is predicted to be remarkably quiet with respect to regulation limits as well as to other aircraft. Cumulative margins to Chapter 14 and Chapter 4 limits are predicted to be 27.4 and 53.1 EPNdB, respectively. Addition of inlet and bypass duct acoustic treatment could drive certification noise levels even lower.

Acknowledgments

This work was performed with support from NASA's Advanced Air Transport Technology Project. Thanks also go to NASA Glenn Research Center's Daniel L. Sutliff and Clifford A. Brown for providing DGEN 380 acoustic measurements and to Joseph W. Connolly and Yuan Liu at NASA for providing the DGEN engine performance data used in this report.

References

[1]NASA Space Act Agreement SAA3-1370, "Acoustic Testing of Price Induction DGEN 380 Turbofan Jet Engine," June, 2014.

[2]"The Little Engine that Could," NASA Press Release, 2014 [URL: http://www.nasa.gov/content/the-little-engine-that-could/, accessed March, 2015].

[3]International Standards and Recommended Practices – Environmental Protection, "Annex 16 to the Convention on International Civil Aviation, Volume I: Aircraft Noise," 7th Edition, International Civil Aviation Organization (ICAO), Montreal, Canada, July 2014.

[4]U.S. Code of Federal Regulations, Title 14, Chapter I, Part 36, "Noise standards: Aircraft Type and Airworthiness Certification."

[5]Gillian, R.E.: "Aircraft Noise Prediction Program User's Manual," NASA TM-84486, 1983.

[6]Zorumski, W.E.: "Aircraft Noise Prediction Program Theoretical Manual, Parts 1 and 2," NASA TM-83199, 1982; Currently maintained at NASA Langley by the ANOPP team in electronic format and provided upon request; Latest revision: Level 30.

[7]Emmerling, J.J.; Kazin, S.B.; and Matta, R.K.: "Core Engine Noise Control Program. Volume III, Supplement 1 - Prediction Methods," FAA-RD-74-125, III-I, Mar. 1976 (Available from DTIC as AD A030 376).

[8]Heidmann, M.F.: "Interim Prediction Method for Fan and Compressor Source Noise," NASA TMX-71763, 1979.

[9]Krejsa, E.A.; and Stone, J.R.: "Enhanced Fan Noise Modeling for Turbofan Engines," NASA CR-2014-218421, 2014.

[10]Stone, J.R.; Krejsa, E.A.; Clark, B.J.; and Berton, J.J.: "Jet Noise Modeling for Suppressed and Unsuppressed Aircraft in Simulated Flight," NASA TM-2009-215524, 2009.

[11]Fink, M.R.: "Airframe Noise Prediction Method," FAA-RD-77-29, March, 1977.

[12]Maekawa, Z.: "Noise Reduction By Screens," *Memoirs of the Faculty of Engineering*, Vol. 12, Kobe University, Kobe, Japan, 1966, pp. 472-479.

[13]Bendat, Julius S.; and Piersol, Allan G.: "Engineering Applications of Correlation and Spectral Analysis," Wiley-Interscience, New York, NY, 1980.

[14]European Aviation Safety Agency: Type Certificate Data Sheets, Noise [URL: https://easa.europa.eu/document-library/noise-type-certificates-approved-noise-levels, accessed March, 2015].